FLORIDA STATE UNIVERSITY

COLLEGE OF ARTS AND SCIENCES

UNCERTAINTY IN SCATTEROMETER-DERIVED VORTICITY

By

KELLY McBETH FORD

A Thesis submitted to the
Department of Meteorology
in partial fulfillment of the
requirements for the degree of
Master of Science

Degree Awarded:

Fall Semester, 2008

The members of the Committee approve the Thesis of Kelly McBeth Ford defended on August 14, 2008.

_____
Mark Bourassa
Professor Directing Thesis

_____
Paul Reasor
Committee Member

_____
Philip Cunningham
Committee Member

The Office of Graduate Studies has verified and approved the above named committee members.

ACKNOWLEDGEMENTS

TABLE OF CONTENTS

LIST OF FIGURES

ABSTRACT

A more versatile and robust technique is developed for determining surface vorticity based on vector winds from the SeaWinds scatterometer on the QuikSCAT satellite. The improved technique is discussed in detail and compared to two previous studies by Sharp et al. (2002) and Gierach et al. (2007) that focused on early development of tropical systems. The error characteristics of the technique are examined in detail. Specifically, three independent sources of error are explored: random observational error, truncation error and representation error. Observational errors are due to random errors in the observations. It is estimated as a worst-case scenario and the vorticity observational uncertainty, expressed as one standard deviation, is approximately 0.5×10^{-5} s^{-1} for the current method. Truncation error associated with the assumption of linear changes between wind vectors is more complicated, thus for accurate results it must be estimated on a case-by-case basis. An attempt is made to determine a lower bound of truncation errors, through the use of composites of tropical disturbances. This lower bound is calculated as 10^{-7} s^{-1} for the composites, which is relatively small compared to the tropical disturbance detection threshold set at 5×10^{-5} s^{-1}, used in an earlier study. The third type of error discussed is due to the size of the area being averaged. If a vorticity maximum is present at the center of this area (away from the edges), it will be missed, resulting in an error. Tropical and sub-tropical low pressure systems from one month of QuikSCAT observations are used to examine this error, resulting in a bias of approximately 1.5×10^{-5} s^{-1} for the comparison of vorticity calculated on a 100 km scale to vorticity calculated on a 25 km scale. The discussion of these errors will benefit future projects of this nature as well as future satellite missions.

CHAPTER 1

INTRODUCTION

The development of tropical systems has been a widely discussed process for centuries. Early research started with Yanai (1968) and McBride and Zehr (1981) who used surface and upper air data to create composites of developing and non-developing tropical systems. These data were extremely limited, thus restrictive to their storm composites. There have been many improvements in observations used for tropical storm analysis and tracking in the last five decades greatly attributed to the development of weather satellites. Geostationary Operational Environmental Satellites (GOES) first launched on Oct. 16, 1975 (e.g., Kossin 2002, Velden et al. 1998, Goerss et al. 1998). For example, gridded analysis and infrared satellite data have been used to broadly categorize observed western North Pacific genesis cases according to the prominent large-scale flow pattern (Ritchie and Holland 1999). In the Atlantic Basin, easterly waves (Carlson 1969; Burpee 1972, 1974, 1975; Reed et al. 1977; Thorncroft and Hoskins 1994 a,b) are related to approximately 63% of tropical cyclones (Avila and Pasch 1992). Recent mesoscale-resolving observations of easterly waves suggest a stochastic genesis process in which mesoscale vortices generated within the elevated cyclonic vorticity environment of the easterly wave interact and organize to form the incipient cyclonic surface circulation (Ritchie and Holland 1997; Simpson et al. 1997). Surface vector winds as measured by the NASA Scatterometer (NSCAT) aboard the Advanced Earth Observing Satellite (ADEOS) on August 16, 1996 led to studies of tropical cyclone genesis. The introduction of QuikSCAT's SeaWinds instrument extensively improved data coverage and availability of ocean surface winds. These new data facilitated research into the potential for earlier identification of likely precursors to tropical depressions (TD) as investigated by Katsaros et al. (2001) and studies (Sharp et al. 2002; Gierach et al. 2007) that directly influenced the research conducted herein. Sharp et al. (2002) developed an objective technique that could potentially be used operationally to identify systems (depressions and disturbances) likely to develop into tropical storms (TS) or hurricanes. Gierach et al. (2007) modified the method developed by Sharp et al. (2002), and applied it in conjunction with GOES IR to track tropical disturbances much farther back in time than aforementioned methods. They found that convection and surface rotation were both found at the earliest

identifiable stages of genesis. A critical component of these studies is the use of near surface winds to examine circulation or rotation.

The main goals of this project are to improve upon the scatterometer-based calculation of vorticity, and to characterize errors in this technique. The major sources of error in the calculation of scatterometer-based surface vorticity are investigated and discussed. The strengths and weaknesses of the new and old methods (that focused on tropical systems) are discussed in terms of the improvements made upon earlier methods as well as considerations of how accuracy might change for prospective satellite missions.

This paper is organized as follows: chapter 2 describes the QuikSCAT SeaWinds data used in this study. Details regarding the methodology of the satellite-based vorticity calculation and comparisons to previous techniques are highlighted in chapter 3. Sources of error including ambiguity selection errors, random vector component errors, truncation errors and representation errors are discussed in chapter 4. Chapter 5 covers opportunities for improvement for future applications. Overall, the detection technique continues to prove successful while reducing error in the results.

CHAPTER 2

SEAWINDS DATA

The QuikSCAT SeaWinds Scatterometer data set used in this study is an updated version similar to that used by Gierach et al. (2007); version-3a of the Ku2001 product developed by Remote Sensing Systems (RSS). The data set includes time, location, surface (10 m elevation) equivalent neutral wind speed (Ross et al. 1985), wind direction and a rain-flag. Four satellite microwave radiometers are used to determine if rain is present at the location of the QuikSCAT observation, and when no radiometer data are available, the occurrence of adverse influences from rain is statistically estimated from the scatterometer backscatter (Mears et al. 2000). This usage of the rain flagging information is highly conservative. For tropical applications a conservative rain flag appears to be necessary; however, this approach seriously overflags for mid-latitude applications.

A limitation for studies of tropical development is the temporal sampling, which has slightly less than twice daily coverage over the Atlantic basin. In contrast, sampling is much better near the ice caps; however, cyclones tend to propagate very rapidly in these regions. Another key limitation for the calculation of surface vorticity is the spatial grid. QuikSCAT observations have a 25 km grid spacing within a swath that is 1800 km wide (76 vector wind cells across the swath). Therefore, the smallest spatial scale for which vorticity can be calculated is 625 km^2, assuming that the spatial resolution is approximately a point. The actual scatterometer wind cell resolution depends on the processing technique used to convert the observed backscatter to wind vectors; however, it is smaller than the grid spacing (Bourassa et al. 2003). One other limiting factor is degradation of the accuracy of the wind vectors when too large a fraction of the signal returned to the satellite is due to rain (Draper and Long 2004; Weissman et al. 2003, Weissman and Bourassa 2001). The vorticity signatures of tropical systems are often associated with rain; therefore, it is important to develop a technique that is either insensitive to seriously rain contaminated data or (in this case) attempts to avoid using such data.

The domain for this study is the portion of the Atlantic basin from the western coast of Africa to the east coast of North America and the Equator to 30° N. Utilizing this area of the basin allows for most Atlantic tropical systems to be detected as well as limiting interference

with mid-latitude storm systems. This method for determining vorticity can be applied to any basin; however, the detection thresholds for tropical disturbances determined by Gierach et al. (2007) might require some modification.

CHAPTER 3

METHODOLOGIES

The first subsection describes the technique used to calculate vorticity at a range of spatial scales. The second subsection puts this technique in the context of previous techniques used to identify tropical systems. The smoothing required for this approach is much different than required for two previous techniques which are described in the last two subsections.

3.1 Vorticity Calculation

Working with QuikSCAT swath data poses several issues in attempting such a calculation. Swaths are not in a perfectly gridded format and some data points might be missing (due to land contamination or being outside the observational swath) or rain contaminated. To account for this, the calculation technique is developed to work around such points, and outputs a missing value if there are insufficient good data points.

Vorticity (ζ) is calculated at the center of a "shape", as defined by available data in the swath, using the circulation (C) about the shape and divided by the area (A) of the shape.

$$\zeta = \frac{C}{A} \tag{1}$$

The circulation theorem is used to calculate the circulation:

$$C = \oint \mathbf{v} \cdot d\mathbf{l}, \tag{2}$$

where $\mathbf{v}$ is the velocity along the closed contour and $\mathbf{l}$ is an element tangent to the contour. The wind vector components are linearly interpolated between adjacent good observations. Then $\int \mathbf{v} \cdot d\mathbf{l}$ becomes $\sum \mathbf{v} \bullet \mathbf{l}$. An individual dot product in this sum can be calculated as

$$\mathbf{v} \bullet \mathbf{l} = \frac{1}{2}\left(u_2 + u_1, v_2 + v_1\right) \cdot \left(x_2 - x_1, y_2 - y_1\right), \tag{3}$$

where x and y refer to the longitudinal and latitudinal positions (with differences in meters), and u and v are the zonal and meridional components of the surface wind vector. The circulation is the sum of (3), spanning the circumference of the shape.

If the shape is based on only three wind observations, the area (a triangle) is calculated using

$$A = \frac{1}{2}(x_1 - x_0)(y_2 - y_0) - (x_2 - x_0)(y_1 - y_0) \qquad (4)$$

If four or more points are available, area and vorticity are calculated for a polygon using

$$A = \left| \sum_{m=1}^{n-1} \left[A_0 + x_m (y_{m+1} - y_{m-1}) \right] \right|, \text{ and} \qquad (5)$$

$$A_0 = x_1 (y_2 - y_1) + x_1 (y_1 - y_{n-2}) \qquad (6)$$

where n is the total number of points enclosing the polygon, and the values of x and y are determined relative to the center of mass of the points used in the calculation.

The vorticity is then determined using the circulation from equation (3) and the area from equations (4,5,6). If more than 20% of the vectors on the circumference of the shape are missing (or more than 25% when only 4 points are considered), the vorticity is also set to missing.

3.2 Detection Technique

The tropical disturbance detection method is vorticity-based, with the relative vorticity calculated within the QuikSCAT swath. Vorticity is first calculated for a 'ring' with a diameter of 100 km (termed here on as "ringsize 4"), or four QuikSCAT cells in diameter (Figure 1). At each vorticity point, a test with three components is conducted:

1)   The vorticity must exceed a minimum threshold of 5×10^{-5} s^{-1} as determined by Gierach et al. (2007).
2)   The maximum non-rainflagged wind speed within and on all sides of the ring must exceed 6.3 m s^{-1} (Gierach et al. 2007).
3)   The above criteria must be met for at least 30% of the vorticity points within the ring's area.
4)   Mention cloud cover constraint (and how it is used – or not used – herein.

The second criteria was not altered for this study but may require more finer tuning depending on the application of this method (i.e. tropical system detection or tracking, mid-latitude storm analysis and the basin of interest, etc.). The third point is important for reducing false alarms associated with questionable wind vectors: vectors that perhaps should have been

flagged as seriously rain contaminated, or vectors with large directional errors. When the first two criteria are met, all wind vectors within two QSCAT grid cells, are marked as a potential tropical system. These locations are then examined using the first three criteria, and on spatial scales from 25 km to 250 km. Specifically, these locations are examined with a ringsize ten (a diameter of 250 km, or ten QuikSCAT cells in diameter). The larger spatial scale improves the identification of systems that are too rain contaminated on the 100 km scale (e.g., tropical disturbances nearing the tropical depression stage, or centers of stronger systems). If a tropical system is not identified at a ringsize ten, the ringsize is decreased by one (diameter is reduced by 25 km), and the process is repeated until all three conditions are met or the diameter reaches a size of zero. When all three criteria are met, prior to the test ringsize being reduced to zero, the location is noted as being associated with a tropical system.

a)   b)
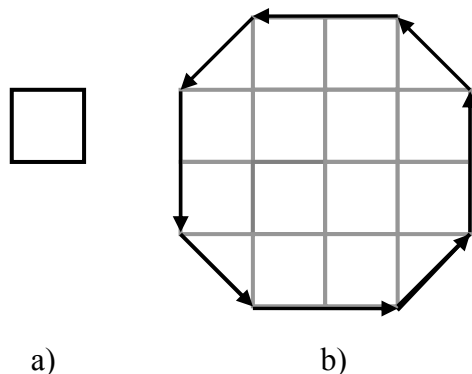
Figure 1. a) Illustration of a ringsize of one (utilized by Sharp et al. 2002 and Gierach et al. 2007) and represents an area 25 km by 25 km or one QuikSCAT cell and b) illustrates a ringsize of four (used in this study) and represents an area 100 km by 100 km or four QuikSCAT cells. For the previous studies (Sharp et al. 2002 and Gierach et al. 2007), vorticity was calculated from wind vectors at the four corners of the box. In the present study, the number of vorticity data points around the perimeter of the ring is increased and can include as many as 12 data points.

3.3 Detection technique developed by Sharp et al. (2002)

Sharp et al. (2002) created the foundation for the research of this study by developing an objective technique that could potentially be used operationally to detect storm systems, in the topical depression or tropical disturbance stage of development, that were likely to develop to TS status or higher. That initial study used SeaWinds observations from the 1999 Atlantic hurricane

season and included the Gulf of Mexico, the Caribbean Sea and the tropical Atlantic Ocean between 10° N and 25° N.

The key differences from the technique described in section 3.2 are in the calculation of vorticity and in smoothing. The spatial area for averaging the vorticity was a 7 by 7 box of scatterometer cells (175 km by 175 km) centered on each vector wind cell in the swath. Individual vorticity values were calculated at the center of a 2 by 2 box of cells. The circulation theorem was used to determine the circulation around each box. and each of these circulations was then divided by the appropriate area. A minimum of three wind vectors were required for this calculation (a triangle replaces the box). The vorticity is then averaged within the 175 km by 175 km, which is similar to the total of the circulations divided by the total of the area. Rainflags were not removed due to smoothing associated with spatial averaging. In order for an average to be calculated from the individual values, it was required that at least 90% of the vorticity calculations within the 7 by 7 box be valid (non-missing). Next, a similar test containing three criteria was conducted:

1) The average vorticity in the 7 by 7 box must exceed $10 \times 10\text{-}5 \text{ s}^{-1}$.

2) The maximum rain-free wind speed within the box must exceed 10 m s^{-1}.

3) The above two criteria must be met at least 25 times within a 350 km by 350 km area centered on the center of circulation.

A serious problem with this technique is that circulation about missing points in the interior also contributed to the estimate of circulation. Consequently, even seriously rain contaminated vectors were used in the vorticity calculation, thereby eliminating rain contamination as a cause of missing vectors. The center of circulation of the systems detected could be no closer to the edge of a swath or a landmass than 150 km. Sharp et al. (2002) determined that this method of detection proved to be successful for both the 1999 and 2000 hurricane seasons and concluded that future operational use might prove beneficial when used in conjunction with traditional methods. Our new technique, applied only with a radius of 175 km, would likely be a more robust calculation because the land constraint could be dropped and rain-flagged vectors are not used in the calculation, nor would interior circulations contribute to the total.

3.4 Detection technique modified by Gierach et al. (2007)

Gierach et al. (2007) adapted the method developed by Sharp et al. (2002) and coupled it with GOES IR to track storms during the tropical disturbance stage of development. The technique used by Gierach et al. (2007) averages vorticity within SeaWinds swaths in a 100 km by 100 km area. Individual vorticity values are calculated using the same technique developed by Sharp et al. (2002). Once vorticity is calculated, a similar, but updated, test of four criteria was conducted:

1) The average vorticity in the 100 km by 100 km area must exceed 5×10^{-5} s^{-1}.

2) The maximum rain-free wind speed within the box must exceed 6.3 m s^{-1}.

3) The above two criteria must be met in at least 80 % of the calculated vorticity cells and be within 50 km of the vorticity points being tested.

4) add the cloud cover constraint.

Gierach et al. (2007) determined the vorticity and wind speed thresholds, listed above, based on SeaWinds data from the 1999-2004 Atlantic hurricane seasons. Fifteen storms were chosen because they stemmed from African Easterly Waves (AEW) and each storm developed into either a TS or hurricane, providing a point of reference for tracking their development back in time. GOES IR data were used to monitor these storms during times between QuikSCAT overpasses, allowing for a more accurate tracking technique than was possible from either QuikSCAT or GOES alone. The technique developed herein is an improvement for the same reasons it is an improvement over the Sharp et al. technique.

CHAPTER 4

DISCUSSION OF ERROR

The important sources of error in our methodology stem from (1) observational errors, (2) truncation errors associated with linear interpolation between wind vectors, and (3) mismatches in the spatial averaging scale. It will be shown that the random errors in the vorticity decreases as the ringsize increases but the rate of reduction is relatively small for ringsizes greater than 100 km (a diameter of four QSCAT wind cells). It will also be shown that estimating truncation error through the use of storm composites as developed by Minter et al. (2007) results in a relatively small truncation error. Finally, it is determined that for vorticity in near to a tropical disturbance or depression, the bias (relative to a 25km scale vorticity) associated with the spatial averaging scale increases with increasing ringsize.

4.1 Contributions From Observational Errors

Observational errors include random vector component errors and ambiguity selection errors. Random errors for SeaWinds on QuikSCAT have been assessed through a variety of approaches (Freilich 1997; Stoffelen 1998; Bourassa et al. 2003; Freilich and Vanhoff 2003). These studies typically investigate the random error where there was no gross error in direction related to ambiguity selection.

4.1.1   Random Errors Ignoring Ambiguity Selection

The propagation of Gaussian distributed random errors can be used to estimate the contribution of observational errors to uncertainty (expressed as a standard deviation) in vorticity. For a variable (y) that is a function (f) of one or more independent variables (x_i), this function can be described in very general terms as

$$y = f(x_1, x_2, x_3 \cdots).$$
(7)

The uncertainty in y, σ_y, can be determined (eq 8) in terms of the uncertainty in the input variables (x_i), again expressed as standard deviations (Taylor 1980).

$$\sigma_y^{\ 2} = \left(\frac{df}{dy}\sigma_{x_1}\right)^2 + \left(\frac{df}{dy}\sigma_{x_2}\right)^2 + \cdots$$
(8)

Assuming the area A is determined with negligible error (in a percentage sense), as is the random error in distance (ℓ) between the center of footprints. The uncertainty in the vorticity σ_ζ can be calculated as

$$\sigma_\zeta{}^2 = \frac{1}{A}\sigma_C{}^2 .$$ (9)

The uncertainty in circulation (σ_c) is

$$\sigma_C{}^2 = \sum \left(\ell_i \sigma_u\right)^2 ,$$ (10)

where σ_u is the uncertainty in the wind speed, assumed to be 0.6 m s^{-1}. Estimates of random component errors for correctly selected ambiguities are 0.6 m s^{-1} (Freilich et al. 1997) for maximum differences in collocation of 30 minutes and 25 km, to plausibly as low as 0.03 m s^{-1} (Bourassa et al. 2003) for collocation differences <0.5 minutes and 5 km. Assuming the highest error in vector components provides an upper limit for uncertainty in the vorticity, and therefore represents a worst-case scenario.

$$\sigma_C{}^2 = \sigma_u{}^2 \sum \left(\ell_i\right)^2$$ (11)

Consequently,

$$\sigma_C{}^2 = \sigma_u{}^2 \cdot 25km \sum \left(n_1 \cdot 1^2 + n_2 \cdot \sqrt{2}^2\right) ,$$ (12)

where n_1 represents the number of "non-diagonal" components of the area perimeter and n_2 represents the number of "diagonal" components of the area perimeter (Figure 1).

This analysis shows that as ringsize increases, vorticity uncertainty decreases (Figure 2), roughly inversely proportional to the diameter of the area used to calculate the vorticity. For diameters exceeding four grid cells, the decrease in uncertainty is small. Thus, choosing a ringsize larger than four would result in only slightly lower levels of uncertainty but would negatively affect the detection technique's ability to maintain the integrity of smaller scale systems.
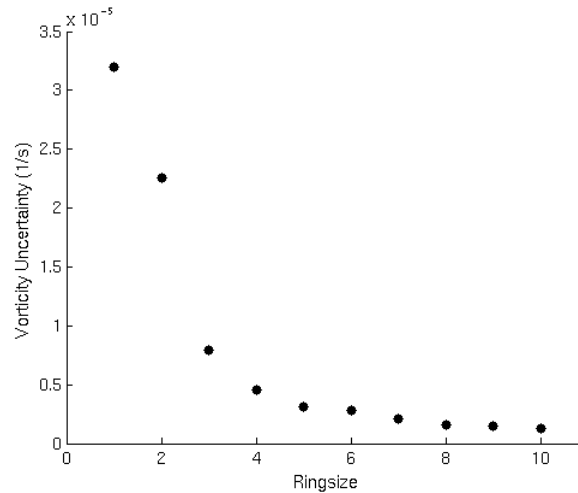
Figure 2. Vorticity uncertainty (s^{-1}, representing one standard deviation) as a function of ringsize. In this study, a ringsize of four is used as error is dramatically reduced while preserving the ability to detect small scale systems. In the two preceding studies by Sharp et al. (2002) and Gierach et al. (2007), a ringsize of one was used with a great deal of additional smoothing.

4.1.2   Ambiguity Selection Error

Ambiguity selection errors are errors associated with selecting the wrong local minima in the best fit of a wind vector to observed backscatter (Naderi et. al 1991, Bourassa et al. 2003). The likelihood of an ambiguity selection error is a function of wind speed, with the chance of such errors being greatest near zero wind speed and diminishing to near zero probability at 8 ms^{-1} (for the RSS product). This model of error suggests that the standard deviation of errors in vorticity might be relatively large for low wind speeds. However, it has also been argued that this dependency on wind speed can be largely explained in terms of random errors in wind vector components, where characterization of these random errors is not a function of wind speed (Freilich 1997). That model for observational errors in wind vectors results in vorticity error characteristics that are independent of wind speed.

The root mean square difference in vorticity, relative to a vorticity with a ringsize 10 (250 km diameter), was calculated for each ringsize (1-9) for increments of wind speed from 0.5 m s^{-1} to 19.5 m s^{-1} increasing by 1.0 m s^{-1} and there was no evidence of a wind speed dependency (Figure 3). This finding indicates that ambiguity selection errors are at most a weak source of observation error in vorticity.
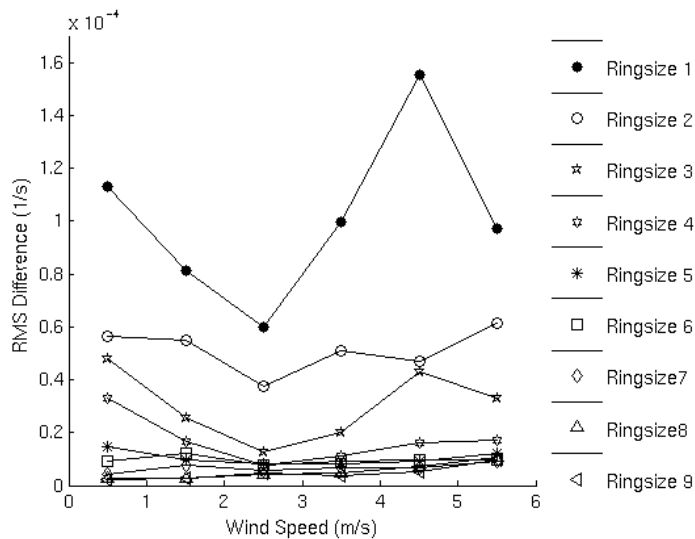
Figure 3. Root mean square error difference versus wind speed (m s^{-1}) for ringsize (i) – ringsize (10). Higher error was expected at low wind speeds if ambiguity selection errors make a substantial contribution to observational errors; however, the results indicate no such trend.

4.2 Truncation Error

The term "ring" is used somewhat loosely, as wind vector spacing only allows a roughly circular shape (Fig. 1) composed of a series of straight edges. An assumption is made that the wind speeds change linearly along the segments of the ring. The error in this assumption is related to higher order changes and the grid spacing. The actual changes of wind speed along the segment can be substantially non-linear. For example, centers of strong low pressure systems or poorly organized tropical disturbances. The shape of tropical disturbances varies greatly from system by system as well as in time. There are also problems associated with seriously rain contaminated data that are not rain flagged. Furthermore, if some points in the ring perimeter are considered bad points (e.g., land or seriously rain contaminated) then there will be an atypically long line segment joining the neighboring points. This situation can greatly increase truncation errors.

Truncation error associated with the assumption of linear changes between wind vectors is complicated, thus for accurate results it must be estimated on a case-by-case basis. A lower limit on the impact of truncation error is determined by examining truncation error based on

13

composite fields of tropical disturbances. These composites were developed by Minter et al. (2007). The composites are much smoother than individual storms that occur in nature. The composites were split into nine stages of development, where the first was essentially a tropical wave, and the last was a TD. Individual storms were based on a blend of QuikSCAT and National Center for Environmental Prediction (NCEP) numerical model analyses using a version of the blending algorithm(adapted from Pegion et al. 2000) that was modified for use with NCEP analyses (Morey et al. 2005; Minter et al. 2007) and constructed with a 1/8 degree grid spacing. Ring diameters from 25 km to 100 km were examined with the QSCAT grid spacing of 25 km, and simulated grid spacing of 12.5 km, 8 1/3 km, and 6.25 km (25 times 1, 1/2, 1/3, and 1/4). Differences were taken between matching points (the locations matching points points on the 25 km grid).

The above approach to estimating truncation error results in a rather small random error for the composite disturbance field. The values are approximately 10^{-7} s^{-1} for a single standard deviation of random errors, which is an order of magnitude less than the estimated observational errors. For real world examples (which contain much less smooth fields), it can be assumed that the errors will be considerably larger, but at this time it is very difficult to assess how much larger.

Assuming that the error statistics are approximately the same for each segment along the edges of the shape (be it a triangle, square or polygon), the total variance associated with random errors in the circulation around the shape (σ_c^2) is approximately proportional to the number of segments times the square of the truncation error uncertainty (σ_T^2) of each segment. In the following example, this number of segments is approximated as the number of points in the perimeter of a circle of diameter n vector wind cells of width Δx.

$$\sigma_c^2 = \sigma_T^2 \ \pi \ n \tag{13}$$

It is also assumed that the error associated with the area calculation is considerably smaller as compared to the magnitude of the error in the circulation, and is ignored. The uncertainty in vorticity (σ_ς) associated with truncation errors is then equal to the uncertainty in circulation divided by the area about which the circulation is calculated. If Δx is the grid spacing of the vector wind observations, then the uncertainty has the following functional form.

$$\sigma_{\varsigma} = \frac{\sigma_T \left(\pi \cdot n \right)^{0.5}}{\pi \, \Delta x^2 \, n^2 / 4} \tag{14}$$

The uncertainty related to truncation error is roughly proportional to the square of the length of each segment, which is roughly proportional to Δx. Therefore, σ_ζ is proportional to n^{-2}, which will decrease with increasing ring size faster than observational error by a factor of n. For any set diameter expressed as a distance (e.g., 100 km), $n\Delta x$ will be constant, hence σ_ζ for a specific spatial scale is proportional to $(\Delta x)^2$: finer grid spacing will greatly reduce truncation errors.

4.3 Representation Error

Spatial averaging errors come in to play when there is a vorticity maximum within (but not touching or only partially touching) the ring used in the vorticity calculations. The larger the ringsize, the more potential there is for a localized vorticity maxima to be reduced. If there is a vorticity maxima at a point within the ring (away from the edges), and is surrounded by vorticity values of lesser magnitude, the maxima is completely missed. In the case of cyclonic systems, representation error tends to result in a negative bias (and underestimation of positive vorticity).

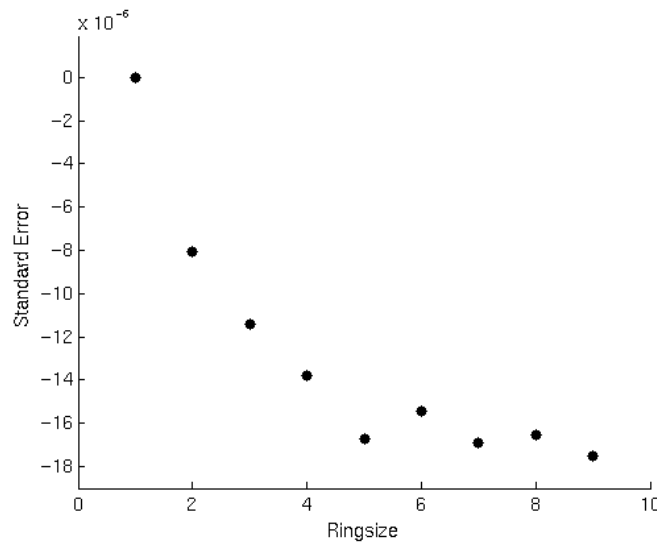Tropical disturbances from 01 August 1999 through 31 October 1999 were examined to

Figure 4. Plot of ringsize (i) – ringsize (1) illustrating spatial averaging scale biases. As the ringsize increases, the area over which the vorticity is averaged increases. This enlargement in area enhances the bias in the vorticity by "smoothing" possible vorticity maxima as shown above.

estimate the bias and random errors associated with representation errors. These are systems typical of our applications. The bias (Figure 4) shows the change in vorticity (centered at the same point) relative to the vorticity with diameter of 25 km. The bias increases as ringsize increases, with a bias of approximately $1.5 \times 10^{-5} \, s^{-1}$ for a diameter of 100 km. The magnitude of the bias doesn't decrease much beyond a ringsize four, thus choosing a ringsize higher than four wouldn't drastically increase the bias from this area assumption. The bias typical of TDs ($1.5 \times 10^{-5} \, s^{-1}$) doesn't largely impact the application of finding tropical disturbances since the detection threshold is more than three times larger ($5 \times 10^{-5} \, s^{-1}$). Different biases will be typical of other types of weather (e.g., fronts or high pressure systems), and therefore the shown biases should not be assumed to apply to all situations.

CHAPTER 5

OPPORTUNITIES FOR IMPROVEMENT AND APPLICATION

As indicated in section 4, errors in the SeaWinds dataset, and approximations due to characteristics of the dataset (e.g., grid spacing), are important considerations when dealing with applications that are sensitive to these errors. Improvements in related satellite technology could do wonders for future applications of this technique. The original scope of the project that supported this work was to improve the calculated scatterometer-derived vorticity, increase the understanding of tropical cyclone genesis or lack of genesis. With improved technology, this detection technique has the potential to contribute to longer tracking times (identification at an early stage) with fewer errors.

One of the greatest changes is improved temporal sampling due to multiple scatterometers in orbit (currently QuikSCAT and ASCAT, with the Indian scatterometer on OCEANSAT2 expected soon). ASCAT's greatly reduced rain contamination (due to the use of C-Band rather than ku-band) is likely to be a substantial advantage; however, this is offset by somewhat reduced resolution.

Increased resolution and finer grid spacing (and reduced sensitivity to rain), such as is proposed in the eXtended Ocean Vector Wind Mission (XOVWM), would allow for reductions in truncation error in comparison to calculation with a similar trial diameter. The finer spatial resolution should also result in better estimates of random observational errors, due to close collocations, which will also reduce our overestimation of the observational errors. Alternatively, the trial storm diameter could be reduced, (without increasing noise) to provide significant decreases in biases (representation errors). The choice tradeoff between reduced bias and reduced random errors would depend on the specifics of the application. For example, the application of forecasting transition to named storms (Sharp et al., 2002) has different requirements than the early detection of tropical disturbances (Gierach et al. 2007). The method developed by Sharp et al. (2002) might not benefit from smaller spatial scales since this would increase random, whereas the reduction of noise in larger scale estimates might make the forecasts more accurate.

CHAPTER 6

CONCLUSION

The improved calculation of scatterometer-based vorticity developed herein can be used for tropical system detection such as those demonstrated by Sharp et al. (2002) and Gierach et al. (2007) as well as studies of vorticity at other latitudes. Improvements include a more accurate calculation of area, a better handling of missing data (due to rain contamination flags, land, and swath edges), characterization of the key sources of error, and a great decrease in the processing time. An understanding of the trade offs between averaging area and noise should be useful for all vorticity based applications. The spatial averaging scale of the vorticity calculation is very easily adjusted from the native grid spacing up to an arbitrarily large size within the observational swath. This versatility makes it easy for a spatial scale to be chosen to match the needs of the application, or for a range of spatial scales to be considered. In the case of tropical disturbances, the range of spatial scales is highly useful for the identification of circulations when there is a great deal of serious rain contamination.

The error characteristics of the vorticity calculation can be described in terms or three types of errors: random observational error, truncation error associated with linear interpolation between wind vectors, and mismatches in the spatial averaging scale (representation errors). The random observational error can be characterized in terms of an isotropic random vector error, the number of observations defining the perimeter of the area, and size of the area. This random error has a standard deviation that is approximately proportional to the random vector error, the radius of the area raised to the -1.5 power, and grid spacing to the 0.5 power. That is, larger areas decrease the random error, and finer grid spacing along the perimeter increases the number of data points and hence increases the random error. It also appears that ambiguity selection errors are adequately described by the random vector component errors, and do not need to be considered as an additional source of uncertainty.

Truncation errors are based upon the linear interpolation between grid points along the perimeter of the ring. The uncertainty in the truncation error is proportional to the square of the distance over which the interpolation occurs; therefore, the larger the distance between valid observations (non-missing and non-rain contamination flagged wind vectors) the larger the error. However, through the use of tropical storm composites as provided by Minter et al. (2007), the

18

lower limit of random error is approximately 10^{-7} s^{-1}. It is impossible at this time to determine truncation error for real world examples due to limited data sources; however, it is substantially larger than this estimate.

Representation errors result in a negative bias when sampling cyclonic systems. This bias is substantial in comparison to the vorticity thresholds used in the Sharp et al. (2002) and Gierach et al. (2007) techniques. These thresholds are empirically chosen to match the spatial smoothing with the objective, and will likely have to be adjusted to account for the differences in smoothing in the techniques for calculating vorticity, particularly if the spatial scales are adjusted. This problem is of reduced importance for the tropical disturbance application because the organization and vorticity of larger spatial scale systems tends to be larger than for smaller scale systems.

REFERENCES

Avila, L. A., and R. J. Pasch, 1992: Atlantic Tropical Systems of 1991. *Mon. Wea. Rev.*, **120**, 2688–2696.

Bourassa, M. A., D. M. Legler, J. J. O'Brien and S. R. Smith, 2002: SeaWinds Validation with Research Vessels. *J. Geophys. Res.,* **108**, DOI 10.1029/2001JC001081.

Burpee, R. W., 1972: The Origin and Structure of Easterly Waves in the Lower Troposphere of North Africa. *J. Atmos. Sci.*, **29**, 77–90.

_____, 1974: Characteristics of North Africa Easterly Waves During the Summers of 1968 and 1969. *J. Atmos. Sci.*, **31**, 1556–1570.

_____, 1975: Some Features of Synoptic-Scale Waves Based on Compositing Analysis of GATE Data. *Mon. Wea. Rev.*, **103**, 921–925.

Carlson, T. N., 1969: Some Remarks on African Disturbances and Their Progress Over the Tropical Atlantic. *Mon. Wea. Rev.*, **97**, 716–726.

Draper, D. W., and D. G. Long, 2004: Simultaneous wind and rain retrieval using SeaWinds data. *IEEE Trans. Geosci. Remote Sens.*, **42**, 1411-1423.

Ebuchi, N., H. C. Graber and M. J. Caruso, 2002: Evaluation of Wind Vectors Observed by QuikSCAT/SeaWinds Using Ocean Buoy Data. *J. Atmos. Oceanic Technol.*, **19**, 2049-2062.

Farrell, B. and M. Montgomery, 1993: Tropical Cyclone Formation. *J. Atmos. Sci.*, **50**, 285-310.

Freilich, M. H., 1997: Validation of Vector Magnitude Datasets: Effects of Random Component Errors. *J. Atmos. Oceanic Technol.*, **14**, 695-703.

_____, M. H. and B. A. Vanhoff, 2003: The Relationship between Winds, Surface Roughness, and Radar Backscatter at Low Incidence Angles from TRMM Precipitation Radar Measurements. *J. Atmos. Oceanic Technol.,* **20**, 549-562.

Gierach, M. M., M. A. Bourassa, P. Cunningham, J. J. O'Brien and P. D. Reasor, 2007: Vorticity-Based Detection of Tropical Cyclogenesis, *J. Applied Meteor. And Climatol.*, **46**, 1214-1229.

Goerss, J. S., Velden, C. S., Hawkins, J. D., 1998: The Impact of Multispectral GOES-8 Wind Information on Atlantic Tropical Cyclone Track Forecasts in 1995. Part II: NOGAPS Forecasts, *Mon. Wea. Rev.*, **126**, 1219–1227.

Katsaros, K. B., E. B. Forde, P. Chang and W. T. Liu, 2001: QuikSCAT's SeaWinds facilitates early identification of tropical depressions in 1999 hurricane season. *Geophys. Res. Lett.*, **28**, 1043-1046.

Kossin, J. P. 2002, Daily Hurricane Variability Inferred from GOES Infrared Imagery. *Mon. Wea. Rev.*, **130**, 2260–2270.

McBride, J. and R. Zehr, 1981: Observational Analysis of Tropical Cyclone Formation. Part II: Comparison of Non-Developing versus Developing Systems. *J. Atmos. Sci.*, **38**, 1132-1151.

Mears, C. A., D. K. Smith, and F. J. Wentz, 2000: Detecting rain with QuikScat. IEEE IGARSS 2000 Proceedings, Honolulu, Hawaii, vol. III, 1235-1237.

_____, C. A., F. J. Wentz, and D. K. Smith, 2000: SeaWinds on QuikSCAT normalized objective function rain flag, Product description version 1.2. Remote Sensing Systems, Santa Rosa, CA, 13.

Minter, E., 2007: QuikSCAT-Derived Near-Surface Vorticity During Tropical Cyclogenesis. Masters Thesis, The Florida State University. 119 p.

Morey, S. L., M. A. Bourassa, X. J. Davis, J. J. O'Brien, J. Zavala-Hidalgo, 2005: Remotely Sensed Winds for Episodic Forcing of Ocean Models. *J. Geophys. Res.*, **110**, 10024, doi:10.1029/2004JC002338.

Naderi, F. M., M. H. Freilich, and D. G. Long, 1991: Space borne radar measurements of wind velocity over the ocean—An overview of the NSCAT scatterometer system. *Proc. IEEE,* **79,** 850–866.

Norquist D. C., E. E. Recker, and R. J. Reed, 1977: The Energetics of African Wave Disturbances as Observed During Phase III of GATE. *Mon. Wea. Rev*, **105**, 334–342.

Pegion, P. J., M. A. Bourassa, D. M. Legler, and J. J. O'Brien, 2000: Objectively Derived Daily "Winds" from Satellite Scatterometer Data. *Mon. Wea. Rev.*, **128**, 3150 -3168.

Ritchie, E.A. and G.J. Holland, 1997: Scale Interactions During the Formation of Typhoon Irving. *Mon. Wea. Rev.*, **125**, 1377-1396.

_____, 1999: Large-scale patterns associated with tropical cyclogenesis in the western Pacific. *Mon. Wea. Rev.*, **127**, 2027-2043.

Ross, D. B., V. J. Cardone, J. Overland, R. D. McPherson, W. J. Pierson Jr., and T. Yu, 1985: Oceanic surface winds. *Adv. Geophys.*, 27, 101-138.

Sharp, R., M. A. Bourassa and J. J. O'Brien, 2003: Early Detection of Tropical Cyclones Using Seawinds-Derived Vorticity. *Bull. Amer. Meteor. Soc.*, **84**, 879-889.

Simpson, J., E. A. Ritchie, G. J. Holland, J. Halverson, and S. Stewart, 1997: Mesoscale Interactions in Tropical Cyclone Genesis. *Mon. Wea. Rev*, **125**, 2643–2661.

Stoffelen, A., 1998: Toward the true near-surface wind speed: error modeling and calibration using triple collocation. *Journal of Geophysical Research*, **103**, 7755–7766.

Taylor, K. E., 1980: The Roles of Mean Meridional Motions and Large-Scale Eddies in Zonally Averaged Circulations. *J. of Atmos. Sci.,* **37**, 1-19.

Thorncroft, C.D. and B. J. Hoskins, 1994: An Idealized Study of African Easterly Waves I: A Linear View. *Quarterly J. of the Royal Meteor. Soc.,* **120**, 953.

Velden, C. S., Olander, T. L., Wanzong, S., 1998: The Impact of Multispectral GOES-8 Wind Information on Atlantic Tropical Cyclone Track Forecasts in 1995. Part I: Dataset Methodology, Description, and Case Analysis. *Mon. Wea. Rev.*, **126**, 1202–1218.

Weissman, D., M. A. Bourassa and J. Tongue, 2001: Effects of Rain Rate and Magnitude on SeaWinds Scatterometer Wind Speed Errors. *J. Atmos. Oceanic Technol*., **19**, 738-746.

_____, D., M. A. Bourassa, J. Tounge, and J. J. O'Brien, 2003: Calibrating the QuikSCAT/SeaWinds radar for measuring rain over water. *IEEE Trans. Geosci. Remote Sens.*, **42**, 2814-2820.

Yanai, M., 1968: Evolution of a Tropical Disturbance in the Caribbean Sea Region. *J. of the Meteorol. Soc. of Japan*, **46**, 86-109.

BIOGRAPHICAL SKETCH

Kelly Ann McBeth was born on August 23, 1983 in Baltimore, MD to Carol and John McBeth. Kelly has one older sister, Melinda who is pursuing a law degree from The Florida Coastal School of Law in Jacksonville, FL. The other half of her family currently resides in Maryland. Kelly grew up in MD until pulling up roots to move to Florida for college. Kelly has always had a passion for weather and knew she needed to learn more.

Kelly graduated from River Hill High School in June of 2001 with Honors. Next, she went on to pursue her Bachelors of Science degree in Meteorology at The Florida State University in Tallahassee, FL and graduated in May of 2005. Knowing that there was still so much more to learn, Kelly applied and was accepted to the Masters program of the Meteorology Department at FSU where she served as a Teaching Assistant to Professors Ahlquist, Reasor and Ruscher. She was assigned her own Introduction to Meteorology Lab with seventeen undergraduate students and was responsible for generating and administering lab assignments, quizzes and homework.

Kelly transitioned into a Research Assistant position at The Center for Ocean-Atmospheric Prediction Studies (COAPS) beginning in the spring of 2006, where she initiated her research under the guidance and supervision of Dr. Mark A. Bourassa. Kelly is currently residing in Tallahassee, FL, accompanied by her new husband, John, and faithful cat, Nimbus.